Arabian Journal of Chemistry (2016) 9, S893–S900

King Saud University

Arabian Journal of Chemistry

www.ksu.edu.sa
www.sciencedirect.com

ORIGINAL ARTICLE

Efficient synthesis of zinc-containing mesoporous silicas by microwave irradiation method and their high activities in acetylation of 1,2-dimethoxybenzene with acetic anhydride

K. Bachari [a,*], R. Chebout [a], M. Lamouchi [b]

[a] *Centre de Recherche Scientifique et Technique en Analyses Physico-Chimiques (C.R.A.P.C), BP 248, Alger RP 16004, Algiers, Algeria*
[b] *Laboratoire de Catalyse et Environnement, EA 2598, MREI, Université du Littoral-Cote d'Opale, 145, Avenue Maurice Schumann, 59140 Dunkerque Cedex, France*

Received 19 May 2011; accepted 10 September 2011
Available online 17 September 2011

KEYWORDS

Zn-JLU-15 materials;
Microwave irradiation;
Acetylation;
Acetic anhydride;
Catalysis;
The liquid phase;
Temperature-programmed-desorption (TPD) of pyridine;
TEM

Abstract A series of acid zinc-containing mesoporous materials have been synthesized by microwave irradiation method with different Si/Zn ratios (Si/Zn = 100, 65, 15) and characterized by several spectroscopic techniques such as: N_2 physical adsorption, ICP, XRD, TEM, FT-IR and a temperature-programmed-desorption (TPD) of pyridine. The liquid phase of acetylation of 1,2-dimethoxybenzene with acetic anhydride has been investigated over this series of catalysts. In fact, the catalyst Zn-JLU-15 (15) showed bigger performance in the acid-catalyzed acetylation of 1,2-dimethoxybenzene employing acetic anhydride as an acylating agent. Furthermore, the kinetics of the acetylation of 1,2-dimethoxybenzene over these catalysts have also been investigated.

1. Introduction

A novel semi-fluorinated surfactant [FSO-100,$CF_3(CF_2)_4$-$(EO)_{10}$] has been used to synthesize ordered mesoporous silica materials in both strongly acidic and neutral conditions (Meng et al., 2004). Very recently, Du et al. (2008) showed highly efficient synthesis of Fe-containing mesoporous materials by using semi-fluorinated surfactant of FSO-100. The microwave–hydrothermal synthesis of molecular sieves is a relatively new area of research (Laha et al., 2006; Bachari and Lamouchi, 2009a,b; Jhung et al., 2003; Bachari et al., 2011; Tompsett et al., 2006; Park et al., 2004). It offers many distinct advantages over the conventional hydrothermal synthesis. They include rapid heating to crystallization temperature due to volumetric heating, resulting in homogeneous nucleation, fast supersaturation by the rapid dissolution of precipitated gels and eventually

* Corresponding author. Tel./fax: +213 21247406.
E-mail address: bachari2000@yahoo.fr (K. Bachari).
Peer review under responsibility of King Saud University.

Production and hosting by Elsevier

http://dx.doi.org/10.1016/j.arabjc.2011.09.007
1878-5352

a shorter crystallization time compared to conventional autoclave heating (Laha et al., 2006; Bachari and Lamouchi, 2009a,b; Jhung et al., 2003; Bachari et al., 2011; Tompsett et al., 2006; Park et al., 2004). It is also energy efficient and economical (Laha et al., 2006; Bachari and Lamouchi, 2009a,b; Jhung et al., 2003; Bachari et al., 2011; Tompsett et al., 2006; Park et al., 2004). On the other hand, Friedel-Crafts aceylation of aromatic compounds and aromatic heterocyclic compounds is an excellent example of electrophilic substitution catalyzed by acidic or basic catalysts, which has been widely used in the industry for the production of various organic value-added intermediates. Preparation of aromatic ketones has received much attention in the recent years because of their commercial importance as they are being largely used as intermediates in the synthesis of pharmaceuticals (naproxen, dextromethorphan, ibuprofen), dyes, fragrances, and agrochemicals (Franck and Stadelhofer, 1998). Conventionally, these reactions are carried out in the presence of homogeneous catalysts such as $AlCl_3$, and BF_3, strong mineral acids like H_2SO_4, HF, or supported Lewis acid catalysts, using acid chloride or anhydride as an acylating agent (Gore, 1964). Regrettably, the use of the above catalysts in the industry causes a lot of environment related problems as they are highly corrosive in nature and cannot be regenerated for more use. Moreover, the separation of the homogeneous catalysts from the product mixture is hard and often a stoichiometric amount excess of the catalysts is required as the Lewis acid catalysts form a complex with the product ketones, which is then destroyed in the hydrolysis step required for product isolation. To avoid the above environmental associated problems, it is desirable to develop a catalyst process which is stable, environmentally friendly, and recyclable. A class of interesting catalytic systems which has been widely used these days and can eliminate the corrosion and environmental problems is the heterogeneous solid Brönsted acid zeolites and zeotypes molecular sieves, which are highly efficient, sustainable, recyclable, and ecofriendly. Indeed, the acetylation of anisole and 1,2-dimethoxy benzene leads to the synthesis of *p*-acetylanisole and 4-acetylveratrole, which are commercially important products and are being used as the precursors of a sun protector and of a component in an insecticide formulation (Guidotti et al., 2005), respectively. Different catalysts including zeolites (Bachiller-Baeza and Anderson, 2004; Quaschning et al., 2005; Derouane et al., 2000; Raja et al., 2001), heteropoly acids (Kaur et al., 2002; Kozhevnikov, 2003), sulfated metal oxides (Cardoso et al., 2004) and AlSBA-15 (Vinu et al., 2008) have been investigated for the Friedel-Crafts alkylation and acetylation reactions. Indeed, in the present study we have studied the liquid phase of acetylation of 1,2-dimethoxybenzene with acetic anhydride over Zn-JLU-15 catalysts synthesized by microwave irradiation method.

2. Experimental

2.1. Synthesis of the catalysts

Microwave–hydrothermal (M–H) synthesis of Zn-JLU-15 mesoporous molecular sieves with different Si/Zn ratios was performed using a MARS5 (CEM Corp., Matthews, NC, USA) microwave digestion system. This system operates at a maximum power of 1200 W and the power can be varied from 0% to 100% and is controlled by both pressure and temperature to a maximum of 350 psi and 513 K, respectively. A 2.45 GHz microwave frequency was used which is the same as that in domestic microwave ovens. The syntheses were carried out in double-walled digestion vessels which have an inner liner and cover made up of Teflon PFA and an outer strength vessel shell of Ultem polyetherimide. In a typical synthesis, 0.8 g of FSO-100 was dissolved in 30 mL of H_2O, followed by addition of required amount of $Zn(NO_3)_2{\cdot}4H_2O$(Si/Zn molar ratio = 100, 65 and 15). The mixture was stirred at room temperature for 0.5 h. After addition of 1.25 mL of tetraethylorthosilicate (TEOS), the mixture was stirred at room temperature for 96 h. Thus obtained gel was allowed to crystallize under microwave–hydrothermal conditions at 373 K for 2 h. The crystallized product was filtered off, washed with warm distilled water, dried at 383 K and finally calcined at 813 K in air for 6 h.

2.2. Characterization techniques

The X-ray diffraction (XRD) patterns of samples were recorded with a powder XRD instrument (Rigaku D/max 2500PC) with Cu Kα radiation (λ = 0.154 18 nm). It was operated at 40 kV and 50 mA. The experimental conditions correspond to a step width of 0.02° and the scan speed of 10 °C/min. The diffraction patterns were recorded in the 2θ range of 1–10°. Fourier transform infrared spectra of samples were recorded on a Nexus FT-IR 470 spectrometer made by Nicolet Corporation (USA) with KBr pellet technique. The effective range was from 400 to 4000 cm^{-1}. Specific surface area and pore size were measured by using a NOVA2000e analytical system made by Quantachrome Corporation (USA). The specific surface area was calculated by Brunauer–Emmett–Teller (BET) method. Pore size distribution and pore volume were calculated by Barrett–Joyner–Halenda (BJH) method. Transmission electron microscopy (TEM) morphologies of samples were observed on a Philips TEMCNAI-12 with an acceleration voltage of 100–120 kV. The zinc content in the samples was determined by inductively coupled plasma (ICP) technique (Vista-MAX, Varian). The density and strength of the acid sites of the different Zn-JLU-15 samples were determined by the temperature-programmed desorption (TPD) of pyridine. About 100 mg of the materials was evacuated for 3 h at 523 K under vacuum ($P < 10^{-5}$ kPa). Thereafter, the samples were cooled to room temperature under dry nitrogen followed by exposure to a stream of pyridine in nitrogen for 30 min. Subsequently, the physisorbed pyridine was removed by heating the sample to 393 K for 2 h in a nitrogen flow. The temperature-programmed desorption (TPD) of pyridine was performed by heating the sample in a nitrogen flow (50 ml/min) from 393 to 873 K with a rate of 10 K/min using a high-resolution thermogravimetric analyzer coupled with a mass spectrometer (SETARAM setsys 16MS). The observed weight loss was used to quantify the number of acid sites assuming that each mole of pyridine corresponds to one mole of protons.

2.3. Catalytic testing

Acetylation of 1,2-dimethoxybenzene with acetic anhydride has been carried out under liquid phase conditions. The liquid phase reaction set up consists of two necked 50 ml round bottomed flask duly fitted with a condenser in one end for cooling and another vent is closed with Teflon septum for collecting samples by a glass syringe at regular intervals. The whole sys-

tem was kept in a thermostated oil bath attached to a magnetic stirrer coupled with a heating plate. In a typical reaction, 0.1 g of the catalyst was added to a solution of 2.6 g 1,2-Dimethoxybenzene (18.9 mmol), 0.4 g acetic anhydride (3.8 mmol) and 50 ml chlorobenzene together with 1 g nitrobenzene as internal standard. Then, the reaction mixture was heated to the required temperature and the samples were collected at regular intervals of time. The collected samples were analyzed periodically by a gas chromatograph (HP-6890) equipped with a FID detector using a DB-5 capillary column. The products were confirmed with GC-MS (HP-5973) analysis.

3. Results

3.1. Characterization of the samples

The small angle X-ray diffraction patterns of Zn-JLU-15 (Si/Zr = 100, 65, 15) synthesized by microwave irradiation method are shown in Fig. 1. The Zn-JLU-15 (100) sample gives a very strong (100) peak followed by (110) and (200) lower intensity peaks. All three distinct Bragg reflections at low angles were indexed on hexagonal lattice. However, when the zinc content ratio increased from 100 to 15, the intensities of the long range ordered peaks were gradually reduced. The zinc content in Zn-JLU-15 is increased with the Zn content in the synthesis gel (Table 1). The porosity of the samples was evaluated by N_2 adsorption isotherms. Fig. 2 shows the N_2 adsorption–desorption isotherms of the three calcined samples Zn-JLU-15. The specific surface areas and pore size distributions and pore volumes calculated by BET and BJH methods are summarized in Table 1. According to Fig. 2, the N_2 adsorption–desorption isotherms of the two samples Zn-JLU-15 (100) and Zn-JLU-15 (65) exhibit typical type IV isotherms with hysteresis loop caused by capillary condensation

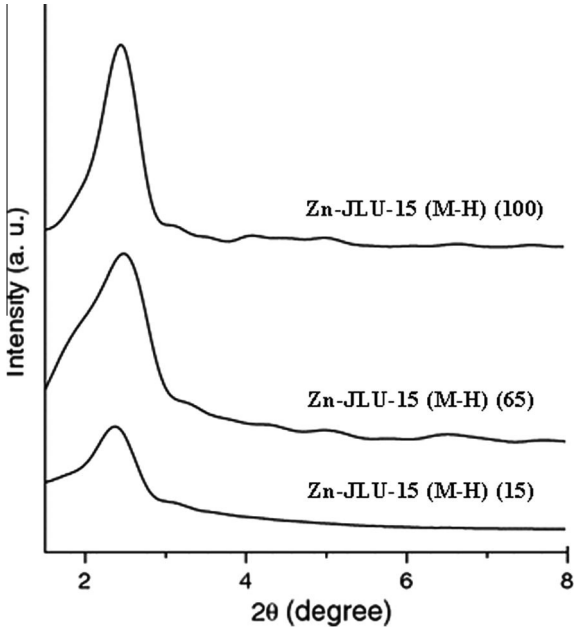

Figure 1 XRD patterns of Zn-JLU-15 materials in the domain of 1–10° (2θ) prepared by microwave–hydrothermal (M–H) process.

in mesopores, manifesting that the two samples possess the obvious mesoporous structure (Bachari and Lamouchi, 2009a). There are three well-defined stages in the isotherms of the two samples that may be identified: the isotherms show a step at the relative pressure (p/p_0) of ca. 0.3–0.4, characteristic of capillary condensation of uniform mesoporous materials, showing that the two samples have uniform pore size distribution and larger pore volume. The isotherms corresponding to $p/p_0 < 0.3$ are due to a monolayer adsorption of nitrogen on the walls of the mesopore. The near horizontal section beyond $p/p_0 > 0.4$ represents the multilayer adsorption on the outer surface of the particles. In addition, from Fig. 2, we can observe that the isotherms of the sample Zn-JLU-15 (100) have a sharper capillary condensation step at the same p/p_0, illustrating that it possesses more uniform pore size distribution as compared with the isotherms of other sample. Moreover, the isotherms of the sample Zn-JLU-15 (15) did not fit into typical type IV isotherms; this is attributed to the partial damage of the mesoporous structure caused by the overfull zinc ions incorporated into the JLU-15 mesoporous molecular sieve. However, combined with the surface area data (693 m^2/g) listed in Table 1 and the XRD data (Fig. 1), the sample Zn-JLU-15 (15) still has a partial mesoporous structure, but the ordering is poor. Fig. 3 presents the pore size distribution curves of the three calcined samples Zn-JLU-15 synthesized by microwave irradiation method. As shown in Fig. 3, narrow and sharp peaks can be observed in a pore size range of ca. 2–3 nm for the samples Zn-JLU-15 (100) and Zn-JLU-15 (65), and the intensity of the peak also is strong as compared with that of the sample Zn-JLU-15 (15), indicating that the two samples have uniform pore size distribution as well. Additionally, as the zinc content in the sample increased, the intensity of the pore size distribution peak became weak, which reflects that the increase of zinc ions incorporated into the silica framework of JLU-15 mesoporous molecular sieve caused the partial distortion of the mesoporous framework, resulting in the irregular pore size distribution and the poor mesoporous ordering. From Table 1, we can conclude that the specific surface area and pore volume of the resulting samples gradually decreased as the zinc content increased, and the pore size is in the range of 2.5–2.9 nm. Combined with the results of XRD and N_2 adsorption isotherms, it is reasonable to conclude that the mesoporous ordering of the sample Zn-JLU-15 synthesized by microwave irradiation method gradually decreased with the increase of the zinc content incorporated into the mesoporous framework. Fig. 4 presents the FT-IR spectra of the synthesized Zn-JLU-15 (65) sample before and after calcination at 813 K in air for 6 h. As shown in Fig. 4, the band at 3500 cm^{-1} is the characteristic band of the water adsorbed on the sample surface. The bands at 1620–1640 cm^{-1} are aroused by the flexion vibration of the OH bond. The band at 1080 cm^{-1} is from the asymmetric extension vibration of Si–O–Si. The band about 810 cm^{-1} is due to the corresponding symmetric vibration of Si–O–Si bond, while the band at 460 cm^{-1} is assigned to rocking vibration of the Si–O–Si bond. The bands at 2921, 2850 and 1480 cm^{-1} are the characteristic bands of the surfactant alkyl chains. After the sample Zn-JLU-15 (65) was calcined at 813 K in air for 6 h, the bands at 2921, 2850 and 1480 cm^{-1} disappeared, certifying that the template had been effectively removed. The TEM images of the samples Zn-JLU-15 (100) and Zn-JLU-15 (65) are shown in Fig. 5. It is observed that the two samples exhibited the hexagonal arrays

Table 1 Physicochemical properties of different Zn-JLU-15 (M–H) samples.

Sample	Chemical analysis		S_{BET} (m^2/g)	Pore volume (cm^3/g)	Pore diameter (nm)
	Si/Zn (gel)	Si/Zn			
Zn-JLU-15	15	14.8	693	0.66	2.9
Zn-JLU-15	65	64.3	936	0.88	2.7
Zn-JLU-15	100	98.7	1136	0.98	2.6

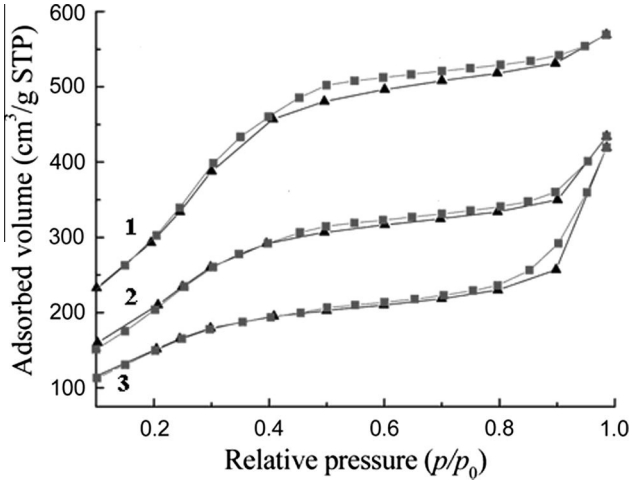

Figure 2 N_2 physical adsorption-desorption isotherms of Zn-JLU-15 materials prepared by microwave–hydrothermal (M–H) process: (1) Zn-JLU-15 (100), (2) Zn-JLU-15 (65), (3) Zn-JLU-15 (15).

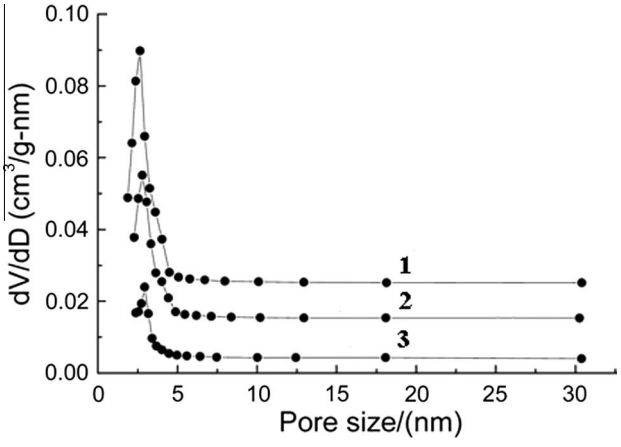

Figure 3 Pore size distribution curves of the of Zn-JLU-15 materials prepared by microwave–hydrothermal (M–H) process: (1) Zn-JLU-15 (100), (2) Zn-JLU-15 (65), (3) Zn-JLU-15 (15).

structure, indicating that the two samples synthesized under microwave irradiation condition possess the mesoporous framework. However, the mesoporous ordering of the sample Zn-JLU-15 (65) is poor as compared with that of the sample Zn-JLU-15 (100). Additionally, it can also be observed that there are not the particles and/or clusters containing zinc species on the surface of the two samples in Fig. 5. Furthermore, the acid site distribution and acid amounts of Zn-JLU-15 synthesized under microwave irradiation condition

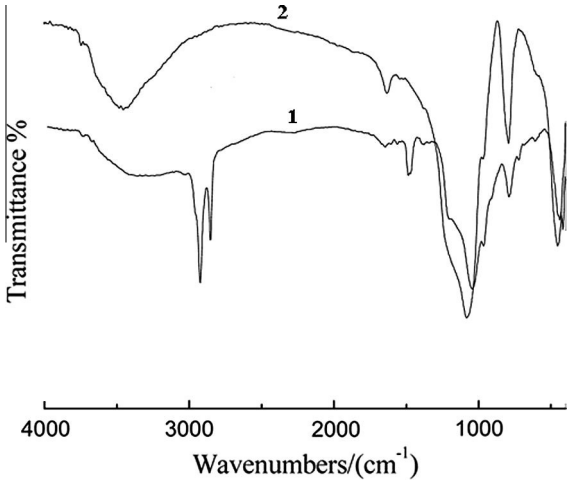

Figure 4 FT-IR spectra of the Zn-JLU-15 (65) material prepared by microwave–hydrothermal (M–H) process: (1) before calcination, (2) after calcinations.

possess were determined using temperature-programmed-desorption (TPD) of pyridine and the data are collected in Table 2. Weak (423 and 633 K), moderate (633–743 K) and strong (> 743 K) acid sites are found in all samples. The weak acid sites are attributed to surface hydroxyl groups and the medium and the strong acid sites originate probably from the incorporation of zinc atoms into the JLU-15 walls. It is interesting to note that the number of weak acid sites decreases with decreasing Si/Zn ratio. However, the amount of medium and strong acid sites decreases with increasing Si/Zn ratio. It should be noted that the total number of acid sites (medium and strong acid sites) of Zn-JLU-15 (15) prepared by microwave–hydrothermal (M–H) is higher than that of Zn-JLU-15 (65) and Zn-JLU-15 (100).

3.2. Catalytic activity

3.2.1. Catalytic performances of Zn-JLU-15 (M–H) materials with different Si/Zn ratio in the acetylation of 1,2-dimethoxybenzene with acetic anhydride

The acetylation of 1,2-dimethoxybenzene has been carried out over Zn-JLU-15 (M–H) materials with different Zn contents (Si/Zn = 100, 65, and 15) using acetic anhydride as an acylating agent. The acetylation of 1,2-dimethoxybenzene with acetic anhydride generates acetic acid in the products, which resulted from the acetic anhydride utilization. Only one product is obtained which is 3,4-dimethoxyacetophenone, due to the fact that both the ortho positions of 1,2-dimethoxybenzene are sterically crowded for electrophilic reaction, acetylation preferentially occurs at the fourth position which is the most favored and para to one of the methoxy substituents. No products

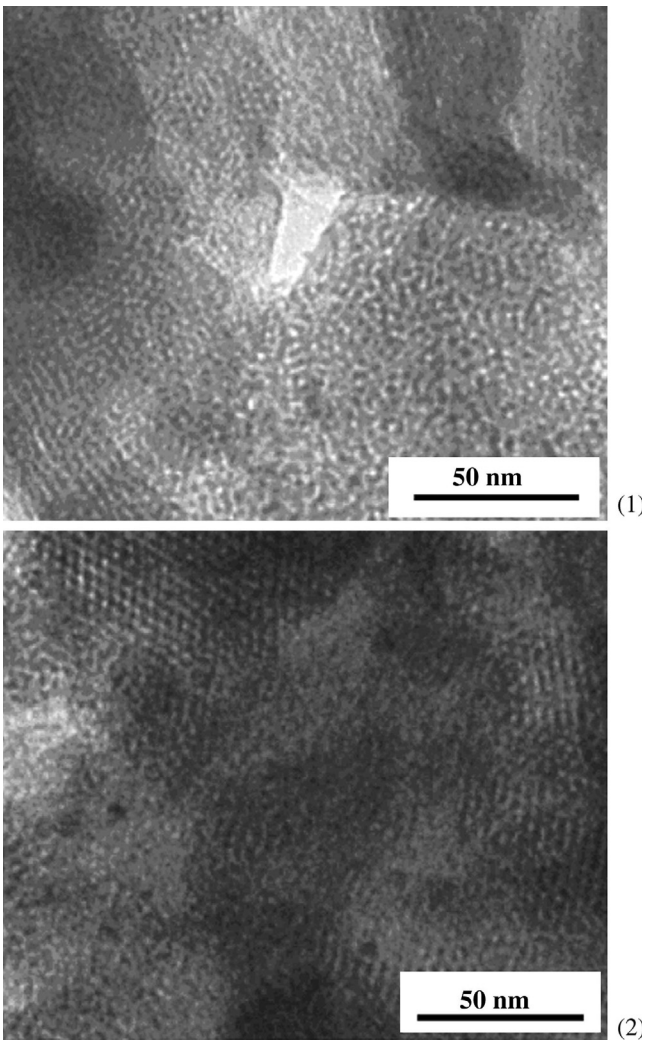

Figure 5 TEM images of the (1) Zn-JLU-15 (65) and (2) Zn-JLU-15 (100) materials prepared by microwave–hydrothermal (M–H) process.

other than 3,4-dimethoxyacetophenone were found in the product mixture. The conversion and the selectivity in the acetylation of 1,2-Dimethoxybenzene over Zn-JLU-15 (M–H) catalysts with different Si/Zn ratio (Si/Zn = 100, 65, and 15) at a reaction temperature of 333 K and under the standard reaction conditions (stoichiometric ratio 1,2DMB/AC = 5, catalyst weight = 0.1 g and a reaction time of 2 h) are given in Table 3. The activity of the catalysts is in the following order: Zn-JLU-15 (M–H) (15) > Zn-JLU-15 (M–H) (65) > Zn-JLU-15 (100). In fact, it is found that Zn-JLU-15 (15) is the mainly efficient catalyst, show much higher conversion of acetic anhydride as compared with that of other catalysts studied. The Zn-JLU-15 (15) catalyst registers the complete acetic anhydride conversion and 100% selectivity to 3,4-dimethoxyacetophenone after 98.4 min of reaction. The very higher activity of Zn-JLU-15 (15) than other Zn-JLU-15 (M–H) catalysts may be mostly attributed by the fact that the catalyst exhibits higher acidity than other Zn-JLU-15 (M–H) catalysts (Table 2). On the other hand, the lower activity of Zn-JLU-15 (M–H) (100) which has the highest surface area and larger pore volume is mainly due to the presence of lower number of active sites on the porous surface. Elsewhere, it was interesting to compare the solids with zeolite catalysts investigated earlier under similar conditions. The activity of the catalysts is in the following order: Zn-JLU-15 (M–H) (15) > BEA > MFI. Indeed, it must be noted that although the acidity of the zeolite catalysts is much higher than that of the Zn-JLU-15 (M-H) (15), the catalytic activity of the latter is superior to that of zeolite catalysts. Thus, it has to be concluded that the accessibility of the active sites by the reactant molecules is higher in Zn-JLU-15 (M-H) (15) than that of the zeolite catalysts, which is supported by their enormous specific surface area and the specific pore volume, and large pore diameter with well-ordered pore structure. These exceptional textural characteristics of the Zn-JLU-15 (M–H) (15) are accountable for its higher catalytic activity and the results further confirm that the catalysts with high surface area, and large pore diameter is highly important for acetylation of substituted aromatic compounds. As the Zn-JLU-15 (M–H) (15) catalyst was found to be highly active, we opt to choose the catalyst for investigating the effect of other reaction parameters such as: the reaction temperature, the stoichiometric ratio 1,2DMB/AC, weight of the catalysts and the recycling of the catalysts on the conversion of acetic anhydride and the selectivity in the acetylation of 1,2-dimethoxybenzene.

3.2.2. The effect of reaction temperature in the acetylation of 1,2-dimethoxybenzene with acetic anhydride

The effect of reaction temperature on the conversion of acetic anhydride in the acetylation of 1,2-dimethoxybenzene over Zn-JLU-15 (M–H) (15) at different reaction time is shown in Table 4. As expected, an increase in the reaction temperature had a favorable effect on the conversion of the acetic anhydride. The conversion of acetic anhydride increases with increasing the reaction temperature. However, the selectivity to 3,4-dimethoxyacetophenone was not changed with increasing the reaction temperature. The selectivity of the product was almost 100% for all the reaction temperature studied. It must be noted that the rate of the reaction at lower temperature is rather slow. On the other hand, at the reaction temperature more than 333 K, the rate of the reaction is very fast. The apparent rate constant of the reaction at different reaction

Table 2 Density and strength of acid sites of Zn-JLU-15 (M–H) catalysts with different Si/Zn ratios (Si/Zn = 100, 65, 15).

Sample	Acid sites (mmol/g)			
	Weak (423–633 K)	Medium (633–743 K)	Strong (743 K)	Total (medium and strong acid sites)
Zn-JLU-15 (15)	0.539	0.191	0.224	0.415
Zn-JLU-15 (65)	0.601	0.123	0.179	0.302
Zn-JLU-15 (100)	0.748	0.107	0.145	0.252

Table 3 The conversion and the selectivity of 1,2-dimethoxybenzene over Zn-JLU-15 (M–H) catalysts with different Si/Zn ratio (Si/Zr = 100, 65, and 15) at a reaction temperature of 333 K, stoichiometric ratio 1,2DMB/AC = 5, catalyst weight = 0.1 g and a reaction time of 2 h.

Sample	Acetic anhydride conversion (%)	Selectivity to 3,4-dimethoxyacetophenone (%)
Zn-JLU-15 (15)	100.0	100.0
Zn-JLU-15 (65)	87.6	100.0
Zn-JLU-15 (100)	64.7	100.0

Table 4 Catalytic activities of Zn-JLU-15 (M–H) (15) at different temperatures: 313, 333 and 353 K, stoichiometric ratio 1,2DMB/AC = 5, catalyst weight = 0.1 g.

Temperature (K)	Time (min)[a]	Selectivity to 3,4-dimethoxyacetophenone (%)	Apparent rate constant k_a ($\times 10^3$ min^{-1})
313	215.0	100.0	11.2
333	98.4	100.0	38.7
353	43.5	100.0	92.3

[a] Time required for complete conversion of acetic anhydride.

Table 5 The conversion and the selectivity in the acetylation of 1,2-dimethoxybenzene over Zn-JLU-15 (M–H) (15) catalyst with different weight of the catalyst at a reaction temperature of 333 K, stoichiometric ratio 1,2DMB/AC = 5.

Weight of the catalyst (g)	Time (min)[a]	Selectivity to 3,4-dimethoxyacetophenone (%)	Apparent rate constant k_a ($\times 10^3$ min^{-1})
0.02	293.0	100.0	7.6
0.1	98.4	100.0	38.7
0.2	60.3	100.0	77.9

[a] Time required for complete conversion of acetic anhydride.

Table 6 The conversion and the selectivity in the acetylation of 1,2-dimethoxybenzene over Zn-JLU-15 (M–H) (15) catalyst with different stoichiometric ratio 1,2DMB/AC at a reaction temperature of 333 K, catalyst weight = 0.1 g.

Stoichiometric ratio 1,2DMB/AC	Time (min)[a]	Selectivity to 3,4-dimethoxyacetophenone (%)	Apparent rate constant k_a ($\times 10^3$ min^{-1})
1	265.3	100.0	9.3
5	98.4	100.0	38.7
10	68.7	100.0	69.6

[a] Time required for complete conversion of acetic anhydride.

temperature was calculated using the pseudo-first-order rate law:

$$\log[1/1-x] = (k_a/2.303)(t-t_0)$$

where k_a is the apparent first-order rate constant, x the fractional conversion of acetic anhydride, t the reaction time and t_0 the induction period corresponding to the time required for reaching equilibrium temperature. A plot of log $[1/1-x]$ as a function of the time gives a linear plot over a large range of acetic anhydride conversions. As expected, the apparent rate constant for the acetylation reaction was increased from $11.2.10^{-3}$ to $92.3.10^{-3}$ min^{-1} with increasing the reaction temperature from 313 to 363 K. The activation energy for the Zn-JLU-15 (15) calculated from an Arrhenius plot was found to be 30.2 kJ mol^{-1}. From these results, it is found that the 333 K is the best temperature for Zn-JLU-15 (15) and is preferred for the subsequent catalytic studies.

3.2.3. The effect of the weight of the catalysts in the acetylation of 1,2-dimethoxybenzene with acetic anhydride

The weight of the catalysts was varied to study its influence on the conversion of acetic anhydride in the acetylation of 1,2-dimethoxybenzene over Zn-JLU-15 (M–H) (15). The weight of the catalysts in the reaction mixture was changed from 0.02 to 0.2 g. Table 5 shows the influence of the weight of the Zn-JLU-15 (M-H) (15) catalyst on the conversion of the acetic anhydride in the acetylation of 1,2-dimethoxybenzene. The concentration of the catalyst in the reaction mixture has a huge impact on the conversion of acetic anhydride. The conversion of the acetic anhydride increases with increasing the weight of the catalyst from 0.02 to 0.2 g at the reaction temperature of 333 K and the stoichiometric ratio 1,2DMB/AC = 5, whereas maintaining 100% selectivity to 3,4-dimethoxyacetophenone. This could be mostly due to the fact that the accessibility of the surface acidic sites is larger at higher catalyst

Table 7 Effect of recycling of the catalyst in the acetylation of 1,2-dimethoxybenzene over Zn-JLU-15 (15) at a reaction temperature of 333 K, stoichiometric ratio 1,2DMB/AC = 5, catalyst weight = 0.1 g.

Catalyst	Time (min)[a]	Selectivity to 3,4-dimethoxyacetophenone (%)	Apparent rate constant k_a ($\times 10^3$ min^{-1})
Fresh	98.4	100.0	38.7
First reuse	99.8	100.0	37.0
Second reuse	100.5	100.0	35.6

[a] Time required for complete conversion of acetic anhydride.

Table 8 Acetylation of different aromatic substrates over Zn-JLU-15 (M–H) (15) catalyst at a reaction temperature of 333 K.

Substituent	Time (min)[a]	Reaction products (selectivity (%))
1,2-dimethoxybenzene	98.4	3,4-dimethoxyacetophenone (100%)
Methoxybenzene (anisole)	38.6	*p*-methoxyacetophenone (98.0%), *o*-methoxyacetophenone (2.0%)
2-methoxy naphthalene	46.3	1-acetyl-2-methoxynaphthalene (97.0%), 6-acetyl-2-methoxynaphthalene (3.0%)

[a] Time required for complete conversion of acetic anhydride.

concentration, which supports the increase in the conversion of acetic anhydride.

3.2.4. The effect of the stoichiometric ratio 1,2DMB/AC on the acetylation of 1,2-dimethoxybenzene with acetic anhydride

The effect of the stoichiometric ratio 1,2DMB/AC on the conversion of acetic anhydride was studied over Zn-JLU-15 (M–H) (15) at a reaction temperature of 333 K as a function of reaction time and the results are shown in Table 6. When the 1,2DMB/AC ratio was varied, the conversion of acetic anhydride was significantly affected. The conversion of acetic anhydride is increased with increasing the 1,2DMB/AC from 1 to 10 at a reaction temperature of 333 K, while the selectivity of 3,4-dimethoxyacetophenone is almost constant in all the cases. It is summarized that the raise of the 1,2DMB/AC ratio may support the adsorption of more amount of 1,2-dimethoxybenzene on the catalysts surface compared to acetic anhydride molecules.

3.2.5. Recycling of the catalysts

The recyclability has been done over Zn-JLU-15 (M–H) (15) in the acetylation of 1,2-dimethoxybenzene at a reaction temperature of 333 K for 2 with 1,2DMB/AC ratio of 5. After the reaction, the catalyst was filtered, washed several times with acetone and dried in an oven at 393 K. Then, the catalyst was activated at 823 K for 6 h under oxygen atmosphere. The recyclability experiments were carried out two times and the procedure for the activation was repeated every time after the reaction. The results on the recyclability are given in Table 7. The catalyst shows approximately similar conversion after two cycles, without any transformation in the selectivity of the products. This shows that the catalyst is very stable under the specified reaction conditions, and is recyclable.

3.2.6. Applications to other aromatic compounds

The acetylation of other substrates with acetic anhydride was accomplished using the Zn-JLU-15 (15) under the optimized reaction conditions. The information of the reaction conditions and the results are presented in Table 8. The catalyst shows good performances in the acetylation of aromatics used in the reaction. In the case of acetylation of methoxybenzene (anisole), it was observed that the time required for complete conversion of acetic anhydride over Zn-JLU-15 (M–H) (15) catalyst is 38.6 min with 98% selectivity to (*p*) 4-methoxyacetophenone, while the rest is (*o*) 2-methoxyacetophenone. The data on the acetylation of 2-methoxynaphthalene with acetic anhydride under nitrobenzene as solvent are also presented in Table 8. In fact, the selectivity to 1-acetyl-2-methoxynaphthalene and 6-acetyl-2-methoxynaphthalene of 97% and 3%, respectively, was showed. The formation of the sterically hindered but kinetically favored product, 1-acetyl-2-methoxynaphthalene has been also shown for the zeolite catalysts with more external surface area and the proton exchanged MCM-41 catalyst at low reaction temperature because position 1 is considered to be the most activated one (Kantam et al., 2005; Andy et al., 2000). Therefore, we consider the preferential formation of 1-acetyl-2-methoxynaphthalene in the Zn-JLU-15 (M–H) catalysts system could be mostly due to the fact that the materials possess high surface area, pore volume and large pore diameter which quite support the formation of the kinetically favored 1-acetyl-2-methoxynaphthalene than that of thermodynamically favored 6-acetyl-2-methoxynaphthalene.

4. Conclusion

Ordered hexagonal Zn-JLU-15 mesoporous molecular sieves with high specific surface area were successfully synthesized via microwave irradiation method. After calcination, the template was effectively removed. The Si/Zn molar ratio is a key factor influencing the textural properties and structural regularity of Zn-JLU-15 mesoporous molecular sieves. High zirconium content is unfavorable to the formation of the Zn-JLU-15 with highly ordered mesoporous structure. These samples have many medium acid sites. The study of the liquid phase of acetylation of 1,2-dimethoxybenzene and other two aromatic compounds with acetic anhydride using Zn-JLU-15 solids shows that these catalysts explain remarkable activities and can also be reused in these reactions for several times.

References

Andy, P., Garcia-Martinex, J., Lee, G., Gonzalez, H., Jones, C.W., Davis, M.E., 2000. J. Catal. 192, 215.

Bachari, K., Lamouchi, M., 2009a. J. Cluster Sci. 20, 573.

Bachari, K., Lamouchi, M., 2009b. Trans. Metal Chem. 34, 529.

Bachari, K., Guerroudj, R.M., Lamouchi, M., 2011. React. Kinet. Mech. Catal. 102, 219.

Bachiller-Baeza, B., Anderson, J.A., 2004. J. Catal. 228, 225.

Cardoso, A.M., Alves Jr., W., Gonzaga, A.R.E., Augiar, L.M.G., Andrade, H.M.C., 2004. J. Mol. Catal. A 209, 189.

Derouane, E.G., Crehan, G., Dillon, C.J., Bethell, D., He, H., Abd Hamid, S.B., 2000. J. Catal. 194, 410.

Du, Y., Liu, S., Ji, Y., Zhang, Y., Liu, F., Gao, Q., Xiao, F.-S., 2008. Catal. Today 131, 70.

Franck, G., Stadelhofer, J.W., 1998. Industrial Aromatic Chemistry. Springer-Verlag, Berlin.

Gore, P.H., 1964. In: Olah, G.A. (Ed.), . In: Friedel Crafts and Related Reactions, vol. III. Wiley Interscience, New York, p. 72.

Guidotti, M., Canaff, C., Coustard, J.M., Magnoux, P., Guisnet, M., 2005. J. Catal. 230, 375.

Jhung, S.H., Chang, J.-S., Hwang, J.S., Park, S.-E., 2003. Microporous Mesoporous Mater. 64, 33.

Kantam, M.L., Ranganath, K.V.S., Sateesh, M., Kumar, K.B.S., Choudary, B.M., 2005. J. Mol. Catal. A: Chem. 225, 15.

Kaur, J., Griffin, K., Harrison, B., Kozhevnikov, I.V., 2002. J. Catal. 208, 448.

Kozhevnikov, I.V., 2003. Appl. Catal. A: General 256, 3.

Laha, S.C., Kamalakar, G., Glaser, R., 2006. Microporous Mesoporous Mater. 90, 45.

Meng, X., Di, Y., Zhao, L., Jiang, D., Li, S., Xiao, F.-S., 2004. Chem. Mater. 16, 5518.

Park, S.-E., Chang, J.-S., Hwang, Y.K., Kim, D.S., Jhung, S.H., Hwang, J.-S., 2004. Catal. Survey Asia 8, 91.

Quaschning, V., Deutsch, J., Druska, P., Lieske, H.J., 2005. J. Catal. 231, 269.

Raja, T., Singh, A.P., Ramaswamy, A.V., Finiels, A., Moreau, P., 2001. Appl. Catal. 211, 31.

Tompsett, G., Conner, W.C., Yngvesson, K.S., 2006. Chem. Phys. Chem. 7, 296.

Vinu, A., Justus, J., Anand, C., Sawant, D.P., Ariga, K., Mori, T., Srinivasu, P., Balasubramanian, V.V., Velmathi, S., Alam, S., 2008. Microporous Mesoporous Mater. 116, 108.